

On the restoration of supersymmetry in twisted two-dimensional lattice Yang-Mills theory

Simon Catterall

Department of Physics, Syracuse University, Syracuse, NY 13244, USA
E-mail: smc@physics.syr.edu

ABSTRACT: We study a discretization of $\mathcal{N} = 2$ super Yang-Mills theory which possesses a single exact supersymmetry at non-zero lattice spacing. This supersymmetry arises after a reformulation of the theory in terms of *twisted* fields. In this paper we derive the action of the other twisted supersymmetries on the component fields and study, using Monte Carlo simulation, a series of corresponding Ward identities. Our results for $SU(2)$ and $SU(3)$ support a restoration of these additional supersymmetries without fine tuning in the infinite volume continuum limit. Additionally we present evidence supporting a restoration of (twisted) rotational invariance in the same limit. Finally we have examined the distribution of scalar field eigenvalues and find evidence for power law tails extending out to large eigenvalue. We argue that these tails indicate that the classical moduli space does not survive in the quantum theory.

KEYWORDS: Lattice, Supersymmetry, Yang-Mills, Kähler-Dirac.

Contents

1. Introduction	1
2. Twisted $\mathcal{N} = 2$ SYM in two dimensions	2
3. Lattice Action and Symmetries	4
4. Twisted Supersymmetries	7
5. Numerical Results	10
5.1 Scalar supersymmetry	10
5.2 The broken supersymmetries	12
5.3 Phase quenching	14
5.4 Thermal boundary conditions	15
5.5 Rotational invariance	16
5.6 Fluctuations of the scalar fields	17
6. Conclusions	18

1. Introduction

Supersymmetric theories have long been of interest to particle physicists both from a phenomenological and theoretical perspective. However for many years the study of such systems on the lattice was problematic. Supersymmetry is typically broken at the classical level in such theories and this makes it difficult if not impossible to construct supersymmetric continuum limits for such theories – see, for example the reviews [1, 2, 3] and references therein.

Recently we have developed a formalism for discretizing supersymmetric theories in D dimensions with $\mathcal{N} = p \times 2^D$, $p = 1, 2, \dots$ supercharges in which one or more supersymmetries are preserved exactly at non-zero lattice spacing.¹ The discretization proceeds from a reformulation of the continuum theory in terms of *twisted* fields. Such a procedure naturally exposes a nilpotent supercharge Q and generically leads to an action which can be written in Q -exact form. These properties allow us to construct supersymmetric lattice actions which preserve the corresponding supersymmetry [4]. Several lattice models have been proposed starting from these twisted continuum formulations [5, 6, 7]. In this paper

¹Strictly the construction yields a lattice theory with complexified lattice fields but theoretical arguments and numerical work have provided evidence that the supersymmetry is retained at the quantum level when the fields are restricted to be real.

we will investigate the discretization developed in [8] and [9]. In this case the resulting lattice theories yield an alternative geometrical reformulation of the orbifold constructions of Kaplan et al. [10]. The explicit connection between the the twisted and orbifold lattice constructions was shown recently by Unsal [11]. The two constructions share the same naive continuum limit and preserve the same number of supersymmetries. Indeed, we show later that linear combinations of the scalar and rank 2 tensor supercharges occurring in the twisted formulation of $\mathcal{N} = 2$ SYM yield, in the naive continuum limit, the conserved nilpotent charge of the equivalent orbifold model. Thus the two approaches to lattice supersymmetry, while differing in their details, depend on essentially the same underlying mechanisms for preserving supersymmetry at finite lattice spacing.

The fermion fields that appear in the twisted formulations can be naturally embedded as components of one or more Kähler-Dirac fields. This geometrical interpretation of the fermions makes it then almost trivial to discretize the theory in a way which avoids the notorious problem of fermion doubling. Furthermore, using the discretization prescription developed in [8], the model may then be studied using numerical simulation techniques [13].

In this paper we extend previous work by deriving the action of the remaining supersymmetries on the twisted fields and use Monte Carlo simulation to examine a series of Ward identities which yield information on the restoration of full supersymmetry in the continuum limit. The next two sections discuss the continuum twisted theory and its transcription to the lattice. We then derive the remaining twisted supersymmetries and go on to describe our numerical results concerning both the Ward identities and the question of the restoration of rotational invariance. The bulk of our simulations are conducted in the *phase quenched approximation* in which any phase of the Pfaffian resulting from integrating the fermions is neglected. We show numerical results indicating that this approximation is likely adequate in the infinite volume continuum limit. We have also conducted simulations employing temporal antiperiodic boundary conditions for the fermions which further suppress the phase fluctuations.

We also show some new results on the distribution of scalar fields in this theory. We argue that the form of this distribution is consistent with a lifting of the classical moduli space via quantum fluctuations. The final section addresses our conclusions.

2. Twisted $\mathcal{N} = 2$ SYM in two dimensions

As discussed in [8] the action of the the two dimensional $\mathcal{N} = 2$ super Yang-Mills theory can be written in the twisted or Q -exact form

$$S = \beta Q \text{Tr} \int d^2x \left(\frac{1}{4} \eta [\phi, \bar{\phi}] + 2\chi_{12} F_{12} + \chi_{12} B_{12} + \psi_\mu D_\mu \bar{\phi} \right) \quad (2.1)$$

where Q is a scalar supercharge obtained by *twisting* the original Majorana supercharges of the theory. The twist consists of decomposing all fields under the action of a twisted rotation group. The latter is obtained as the diagonal subgroup of the direct product of the original (Euclidean) Lorentz symmetry with an $SO(2)$ subgroup of the theory's

R-symmetry. In practice this means that we should treat the Lorentz and flavor indices carried by all fields (and supercharges) as equivalent resulting in a 2×2 matrix structure for the fields. The twisted fields of the theory correspond to the expansion coefficients when this matrix is decomposed on a basis of products of gamma matrices. Explicitly for the supercharge matrix q this decomposition reads

$$q = QI + Q_\mu \gamma_\mu + Q_{12} \gamma_1 \gamma_2 \quad (2.2)$$

while a similar expression for the fermions allows the fermionic content of the theory to be re-expressed in terms of the set antisymmetric tensor fields $(\eta/2, \psi_\mu, \chi_{12})$. The action of the scalar supercharge on the component fields is²

$$\begin{aligned} QA_\mu &= \psi_\mu \\ Q\psi_\mu &= -D_\mu \phi \\ Q\chi_{12} &= B_{12} \\ QB_{12} &= [\phi, \chi_{12}] \\ Q\bar{\phi} &= 2\frac{\eta}{2} \\ Q\frac{\eta}{2} &= \frac{1}{2}[\phi, \bar{\phi}] \\ Q\phi &= 0 \end{aligned} \quad (2.3)$$

Notice that supersymmetry requires the introduction of Q -superpartners with the same tensor structure as the fermions. Carrying out the Q -variation on eqn. 2.1 and subsequently integrating over the field B_{12} leads to the action

$$\begin{aligned} S = \beta \text{Tr} \int d^2x & \left(\frac{1}{4}[\phi, \bar{\phi}]^2 - \frac{1}{4}\eta[\phi, \eta] - F_{12}^2 - D_\mu \phi D_\mu \bar{\phi} \right. \\ & \left. - \chi_{12}[\phi, \chi_{12}] - 2\chi_{12}(D_1 \psi_2 - D_2 \psi_1) - \psi_\mu D_\mu \eta + \psi_\mu [\bar{\phi}, \psi_\mu] \right) \end{aligned} \quad (2.4)$$

The bosonic sector of this action is precisely the usual Yang-Mills action while the fermionic sector constitutes a *Kähler-Dirac* representation of the usual spinorial action [14]. This can be seen explicitly by constructing a Dirac spinor out these twisted fields in the following way

$$\lambda = \begin{pmatrix} \frac{1}{2}\eta - i\chi_{12} \\ \psi_1 - i\psi_2 \end{pmatrix} \quad (2.5)$$

It is straightforward to see that the kinetic terms in 2.4 can then be rewritten in the Dirac form

$$\lambda^\dagger \gamma \cdot D \lambda \quad (2.6)$$

where the gamma matrices are taken in the Euclidean chiral representation

$$\gamma_1 = \begin{pmatrix} 0 & 1 \\ 1 & 0 \end{pmatrix} \quad \gamma_2 = \begin{pmatrix} 0 & i \\ -i & 0 \end{pmatrix} \quad (2.7)$$

²All fields are to be thought of as *antihermitian* matrices in the gauge group.

In the same way the Yukawa interactions with the scalar fields can be written

$$\lambda^\dagger \frac{(1 + \gamma_5)}{2} [\bar{\phi}, \lambda] - \lambda^\dagger \frac{(1 - \gamma_5)}{2} [\phi, \lambda] \quad (2.8)$$

where γ_5 in this representation is

$$\gamma_5 = \begin{pmatrix} 1 & 0 \\ 0 & -1 \end{pmatrix} \quad (2.9)$$

Thus the on-shell twisted action is nothing more than the usual $\mathcal{N} = 2$ SYM action in two dimensions. Indeed, in flat space the twisting process can be thought of as simply a change of variables and is hence fully equivalent to the usual formulation.³

This rewriting of the theory in terms of antisymmetric tensors has two primary advantages – it allows us to formulate the theory on a curved space and as we will show in the next section gives a natural starting point for discretization.

Finally it is worth pointing out that the twisted theory possesses an additional $U(1)$ symmetry inherited from the remaining R-symmetry of the model which is given by

$$\begin{aligned} \psi_\mu &\rightarrow e^{i\alpha} \psi_\mu \\ \chi_{12} &\rightarrow e^{-i\alpha} \chi_{12} \\ \eta &\rightarrow e^{-i\alpha} \eta \\ \phi &\rightarrow e^{2i\alpha} \phi \\ \bar{\phi} &\rightarrow e^{-2i\alpha} \bar{\phi} \end{aligned} \quad (2.10)$$

This symmetry can also be preserved under discretization and ensures the absence of additive mass renormalizations in the theory.

3. Lattice Action and Symmetries

This theory may be discretized by mapping the continuum rank p antisymmetric tensor fields to lattice fields living on p -cubes in a hypercubic lattice and replacing derivatives with appropriate difference operators.

The choice of difference operator is very important to avoid fermion doubling – one must replace $\partial_\mu \rightarrow D_\mu^+$ if the derivative occurs in a curl-like operation and $\partial \rightarrow D_\mu^-$ if the derivative belongs to a divergence [15]. Here, D_μ^+ and D_μ^- refer to the usual forward and backward difference operators respectively. Here gauge covariant versions of these difference operators must be used. We have employed the following definitions [16]:

$$\begin{aligned} D_\mu^+ f(x) &= U_\mu(x) f(x + \mu) - f(x) U_\mu(x) \\ D_\mu^+ f_\nu(x) &= U_\mu(x) f_\nu(x + \mu) - f_\nu(x) U_\mu(x + \nu) \end{aligned} \quad (3.1)$$

³Notice that to make this correspondence and obtain a bounded Euclidean action it is necessary to think of ϕ as a complex matrix which is (minus) the Hermitian conjugate of $\bar{\phi}$.

Notice that these definitions imply that the gauge transformations of lattice scalar, vector and (antisymmetric) tensor fields are

$$\begin{aligned}
f(x) &\rightarrow G(x)f(x)G^\dagger(x) \\
f_\mu(x) &\rightarrow G(x)f_\mu(x)G^\dagger(x+\mu) \\
f_{\mu\nu}(x) &\rightarrow G(x)f_{\mu\nu}(x)G^\dagger(x+\mu+\nu)
\end{aligned} \tag{3.2}$$

where $G(x) = e^{\phi(x)}$ is a lattice gauge transformation and all fields are taken in the adjoint representation. From a lattice perspective these transformations are very natural and correspond to thinking of each field as living on a link running from the origin out to a vertex on the unit hypercube. The definitions of the backward difference operator follow by taking the adjoint

$$\begin{aligned}
D_\mu^- f_{\mu\nu}(x) &= f_{\mu\nu}(x)U_\mu^\dagger(x+\nu) - U_\mu^\dagger f_{\mu\nu}(x-\mu) \\
D_\mu^- f_\mu(x) &= f_\mu(x)U_\mu^\dagger(x) - U_\mu^\dagger(x-\mu)f_\mu(x-\mu)
\end{aligned} \tag{3.3}$$

Notice that this lattice divergence has the merit of demoting the rank of the lattice field as in the continuum and is consistent with the lattice gauge transformation rules listed above.

The final step to constructing the lattice theory is to promote each (anti)hermitian continuum field to a complex lattice field. This allows f and f^\dagger to transform differently under gauge transformations. This in turn is required if we are to construct gauge invariant objects on the lattice. This doubling is actually somewhat natural in a lattice theory with p -form lattice fields since the underlying p -cube with $p > 0$ has two orientations. The complexification of the vector potential $A_\mu^a(x)$ has the additional benefit of allowing the fields $U(x)$ and $U^\dagger(x)$ to vary independently under the twisted supersymmetry. In the end we will require the final path integral be taken along a contour where $U^\dagger U = I$ and the imaginary parts of the gauge field and the fermion fields vanish. This reality condition will allow contact to be made with the usual twisted continuum theory [8, 13].

The Q -exact lattice action now takes the form

$$\begin{aligned}
S_L = \beta Q \text{Tr} \sum_x &\left(\frac{1}{4} \eta^\dagger(x) [\phi(x), \bar{\phi}(x)] + \chi_{12}^\dagger(x) \mathcal{F}_{12}(x) + \chi_{12}(x) \mathcal{F}_{12}(x)^\dagger \right. \\
&\left. + \frac{1}{2} \chi_{12}^\dagger(x) B_{12}(x) + \frac{1}{2} \chi_{12}(x) B_{12}^\dagger(x) + \frac{1}{2} \psi_\mu^\dagger(x) D_\mu^+ \bar{\phi}(x) + \frac{1}{2} \psi_\mu(x) (D_\mu^+ \bar{\phi}(x))^\dagger \right) \tag{3.4}
\end{aligned}$$

This expression will also be Q -invariant if we can generalize the continuum twisted supersymmetry transformations in such a way that we preserve the property $Q^2 = \delta_G^\phi$. The following transformations do the job

$$\begin{aligned}
QU_\mu &= \psi_\mu \\
Q\psi_\mu &= -D_\mu^+ \phi \\
Q\phi &= 0 \\
Q\chi_{12} &= B_{12} \\
QB_{12} &= [\phi, \chi_{12}]^{(12)} \\
Q\bar{\phi} &= \eta \\
Q\eta &= [\phi, \bar{\phi}]
\end{aligned} \tag{3.5}$$

where the superscript notation indicates a *shifted* commutator

$$[\phi, \chi_{\mu\nu}]^{(\mu\nu)} = \phi(x)\chi_{\mu\nu}(x) - \chi_{\mu\nu}(x)\phi(x + \mu + \nu) \quad (3.6)$$

These arise naturally when we consider the infinitesimal form of the gauge transformation property of the plaquette field. Notice that gauge invariance also dictates that we must use the covariant forward difference operator D_μ^+ on the right-hand side of the U_μ variation. The lattice field strength is given by $\mathcal{F}_{\mu\nu}(x) = D_\mu^+ U_\nu(x)$.

Carrying out this lattice Q -variation leads to the following expression for the lattice action

$$\begin{aligned} S_L = \beta \text{Tr} \sum_x & \left(\frac{1}{4} [\phi(x), \bar{\phi}(x)]^2 - \frac{1}{4} \eta^\dagger(x) [\phi(x), \eta(x)] - \chi_{12}^\dagger(x) [\phi(x), \chi_{12}(x)]^{(12)} + B_{12}^\dagger(x) B_{12}(x) \right. \\ & + B_{12}^\dagger(x) \mathcal{F}_{12}(x) + B_{12}(x) \mathcal{F}_{12}(x)^\dagger + \frac{1}{2} (D_\mu^+ \phi(x))^\dagger D_\mu^+ \bar{\phi}(x) + \frac{1}{2} D_\mu^+ \phi(x) (D_\mu^+ \bar{\phi}(x))^\dagger \\ & - \chi_{12}^\dagger(x) D_1^+ \psi_2(x) + \chi_{12}^\dagger(x) D_2^+ \psi_1(x) - \psi_2^\dagger(x) D_1^- \chi_{12}(x) + \psi_1^\dagger(x) D_2^- \chi_{12}(x) \\ & \left. - \frac{1}{2} \psi_\mu^\dagger(x) D_\mu^+ \eta(x) - \frac{1}{2} \eta^\dagger(x) D_\mu^- \psi_\mu(x) + \psi_\mu^\dagger(x) [\bar{\phi}(x), \psi_\mu(x)]^{(\mu)} \right) \end{aligned} \quad (3.7)$$

Finally we must integrate out the multiplier fields B_{12} and B_{12}^\dagger resulting in the term

$$\beta \text{Tr} \sum_x \mathcal{F}_{12}(x)^\dagger \mathcal{F}_{12}(x) \quad (3.8)$$

This can be written

$$\beta \text{Tr} \sum_x \left(2I - U_P - U_P^\dagger \right) + \beta \text{Tr} \sum_x (M_{12} + M_{21} - 2I) \quad (3.9)$$

where

$$U_P = \text{Tr} \left(U_1(x) U_2(x+1) U_1^\dagger(x+2) U_2^\dagger(x) \right) \quad (3.10)$$

resembles the usual Wilson plaquette operator and

$$M_{12}(x) = U_1(x) U_1^\dagger(x) U_2(x+1) U_2^\dagger(x+1) \quad (3.11)$$

Notice that the second term vanishes when the gauge field is restricted to be unitary which is equivalent to requiring $\text{Im} A_\mu(x) = 0$. In this case the action is nothing more than the usual Wilson gauge action.

Having constructed this complexified lattice theory possessing the exact scalar supersymmetry we will subsequently truncate it to the real line by setting the imaginary parts of all fields bar the scalars to zero (the scalars are required to be (anti)hermitian conjugates of each other as in the continuum). In [13] we argued that such a truncation should be valid for the Ward identities associated with the scalar supersymmetry at least for sufficiently large β as a consequence of the Q -exact nature of the action. The numerical results presented in [13] and in this paper are consistent with this.

4. Twisted Supersymmetries

It is straightforward to construct the twisted supersymmetry transformations of the component fields. It follows from the matrix nature of the twist that the continuum fermion kinetic term can be written in the form

$$S_F = \int d^2x \text{Tr} \Psi^\dagger \gamma \cdot D \Psi \quad (4.1)$$

where Ψ corresponds to the matrix form of the Kähler-Dirac field

$$\Psi = \frac{\eta}{2} I + \psi_\mu \gamma_\mu + \chi_{12} \gamma_1 \gamma_2 \quad (4.2)$$

This term is clearly invariant under $\Psi \rightarrow \Psi \Gamma^i$, $i = 1 \dots 4$ where Γ^i are the basis of products of gamma matrices introduced earlier in eqn. 2.2.

Consider first the case $\Gamma^4 = \gamma_1 \gamma_2$. In terms of the component fields the transformation $\Psi \rightarrow \Psi \Gamma^4$ effects a duality map

$$\begin{aligned} \frac{\eta}{2} &\rightarrow -\chi_{12} \\ \chi_{12} &\rightarrow \frac{\eta}{2} \\ \psi_\mu &\rightarrow -\epsilon_{\mu\nu} \psi_\nu \end{aligned} \quad (4.3)$$

Such an operation clearly leaves the Yukawa terms invariant and trivially all bosonic terms. It is thus a symmetry of the continuum action. By combining such a transformation with the original action of the scalar supercharge one derives a additional supersymmetry of the theory – that corresponding to the twisted supercharge Q_{12} . Explicitly this supersymmetry will transform the component fields of the continuum theory in the following way

$$\begin{aligned} Q_{12} A_\mu &= -\epsilon_{\mu\nu} \psi_\nu \\ Q_{12} \psi_\mu &= -\epsilon_{\mu\nu} D_\nu \phi \\ Q_{12} \chi_{12} &= -\frac{1}{2} [\phi, \bar{\phi}] \\ Q_{12} B_{12} &= [\phi, \frac{\eta}{2}] \\ Q_{12} \bar{\phi} &= -2\chi_{12} \\ Q_{12} \frac{\eta}{2} &= B_{12} \\ Q_{12} \phi &= 0 \end{aligned} \quad (4.4)$$

From the Q and Q_{12} transformations it is straightforward to verify the following algebra holds

$$\begin{aligned} \{Q, Q\} &= \{Q_{12}, Q_{12}\} = \delta_\phi \\ \{Q, Q_{12}\} &= 0 \end{aligned} \quad (4.5)$$

where δ_ϕ denotes an infinitesimal gauge transformation with parameter ϕ . This allows us to construct strictly nilpotent symmetries $\hat{Q}_\pm = Q \pm iQ_{12}$ in the continuum theory corresponding to using the (anti)self-dual components of the original Kähler-Dirac field.

In the same way we can try to build an additional supersymmetry by combining the invariance of the fermion kinetic term under $\Psi \rightarrow \Psi\Gamma^1$ with the existing scalar supersymmetry. This effects the following transformation of fermion fields:

$$\begin{aligned}
\frac{\eta}{2} &\rightarrow \psi_1 \\
\chi_{12} &\rightarrow -\psi_2 \\
\psi_1 &\rightarrow \frac{\eta}{2} \\
\psi_2 &\rightarrow -\chi_{12}
\end{aligned} \tag{4.6}$$

However, the Yukawas and bosonic terms are only invariant under such a transformation if we simultaneously make the transformation $\phi \rightarrow -\bar{\phi}$. The resultant explicit action of Q_1 on the component fields is given by

$$\begin{aligned}
Q_1 A_1 &= \frac{\eta}{2} \\
Q_1 A_2 &= -\chi_{12} \\
Q_1 \psi_1 &= -\frac{1}{2}[\phi, \bar{\phi}] \\
Q_1 \psi_2 &= -B_{12} \\
Q_1 \chi_{12} &= -D_2 \bar{\phi} \\
Q_1 B_{12} &= [\bar{\phi}, \psi_2] \\
Q_1 \bar{\phi} &= 0 \\
Q_1 \frac{\eta}{2} &= D_1 \bar{\phi} \\
Q_1 \phi &= -2\psi_1
\end{aligned} \tag{4.7}$$

Similarly the supersymmetry associated with Γ^2 is given by

$$\begin{aligned}
Q_2 A_1 &= \chi_{12} \\
Q_2 A_2 &= \frac{\eta}{2} \\
Q_2 \psi_1 &= B_{12} \\
Q_2 \psi_2 &= -\frac{1}{2}[\phi, \bar{\phi}] \\
Q_2 \chi_{12} &= D_1 \bar{\phi} \\
Q_2 B_{12} &= -[\bar{\phi}, \psi_1] \\
Q_2 \bar{\phi} &= 0 \\
Q_2 \frac{\eta}{2} &= D_2 \bar{\phi} \\
Q_2 \phi &= -2\psi_2
\end{aligned} \tag{4.8}$$

Again, we can verify the following algebra holds

$$\begin{aligned}
\{Q_1, Q_1\} &= \{Q_2, Q_2\} = \delta_{-\bar{\phi}} \\
\{Q_1, Q_2\} &= 0
\end{aligned} \tag{4.9}$$

with $\delta_{-\bar{\phi}}$ a corresponding gauge transformation with parameter $-\bar{\phi}$. This allows us to construct yet another pair of nilpotent supercharges in the continuum theory $\bar{Q}_{\pm} = Q_1 \pm iQ_2$.

It is interesting to check also the anticommutators of these new charges \hat{Q}_{\pm} and \bar{Q}_{\pm} . It is a straightforward exercise to verify the following algebra holds *on-shell*

$$\begin{aligned}\{\hat{Q}_+, \bar{Q}_-\} &= \{\hat{Q}_-, \bar{Q}_+\} = 0 \\ \{\hat{Q}_+, \bar{Q}_+\} &= 4(D_1 + iD_2) \\ \{\hat{Q}_-, \bar{Q}_-\} &= 4(D_1 - iD_2)\end{aligned}\tag{4.10}$$

As an example consider $\{\hat{Q}_+, \bar{Q}_+\}\psi_1$

$$\{\hat{Q}_+, \bar{Q}_+\} = \{Q, Q_1\} - \{Q_{12}, Q_2\} + i(\{Q_{12}, Q_1\} + \{Q, Q_2\})\tag{4.11}$$

Using the component transformations listed above the relevant anticommutators are

$$\begin{aligned}\{Q, Q_1\}\psi_1 &= 2D_1\psi_1 \\ \{Q, Q_2\}\psi_1 &= 2D_1\psi_2 + 2[\phi, \chi_{12}] \\ \{Q_{12}, Q_1\}\psi_1 &= 2D_2\psi_1 \\ \{Q_{12}, Q_2\}\psi_1 &= 2D_2\psi_2 + [\phi, \eta]\end{aligned}\tag{4.12}$$

Thus we find

$$\{\hat{Q}_+, \bar{Q}_+\} = 2D_1\psi_1 - 2D_2\psi_2 - [\phi, \eta] + i(2D_1\psi_2 + 2D_2\psi_1 + 2[\phi, \chi_{12}])\tag{4.13}$$

Using the equations of motion

$$\begin{aligned}-2D_1\psi_1 - 2D_2\psi_2 - [\phi, \eta] &= 0 \\ -2D_2\psi_1 + 2D_1\psi_2 + 2[\phi, \chi_{12}] &= 0\end{aligned}\tag{4.14}$$

we can easily verify the second line of eqn. 4.10. Notice that from these new charges \hat{Q}_{\pm} , \bar{Q}_{\pm} we can build spinorial supercharges of the form

$$\begin{pmatrix} \hat{Q}_+ \\ \bar{Q}_- \end{pmatrix}\tag{4.15}$$

in which case the algebra given in eqn. 4.10 represents the usual supersymmetry algebra in a chiral basis (up to a gauge transformation).

Finally we will be interested in Ward identities which can be derived for a general operator O and take the form

$$\langle Q^i O \rangle = 0 \quad i = 1 \dots 4\tag{4.16}$$

for each of the four supersymmetries. To get nontrivial results the operator O must be gauge invariant and have $U(1)$ charge -1 .

5. Numerical Results

We have implemented the RHMC dynamical fermion algorithm to simulate this lattice theory – for details we refer the reader to [13]. We have examined lattices with L^2 geometry with L in the range 3 – 8 and a variety of lattice couplings. Simulations have been done employing both periodic boundary conditions and thermal boundary conditions corresponding to enforcing antiperiodicity on the fermions in the temporal direction. Following [13] we have worked in the phase quenched ensemble – the Pfaffian arising from integration over the twisted fermions is replaced by its absolute value within the Monte Carlo simulation. We do, however, monitor the phase and in the next section will discuss the results of reweighting our measured observables with those phase fluctuations. Typically, our results derive from $O(10^{3-4})$ trajectories for both $SU(2)$ and $SU(3)$ theories where a single trajectory corresponds to $\tau = 1$ units of classical dynamics time.

5.1 Scalar supersymmetry

Consider first a series of Ward identities associated with the exact lattice supersymmetry Q . The simplest of these corresponds to the statement $\langle S \rangle = -\frac{\partial \ln Z}{\partial \beta} = 0$ reflecting the Q -exact nature of the twisted action. If we integrate out the twisted fermions and the auxiliary field B_{12} we find the following expression for the partition function

$$Z = \beta^{4N_G N_s/2} \beta^{-N_G N_s/2} \int D\phi D\bar{\phi} DU e^{-\beta S_B(\phi, \bar{\phi}, U)} \det(M(\Phi)) \quad (5.1)$$

where N_s is the number of sites and N_G the number of generators of the gauge group. The first prefactor arises from the fermion integration while the second derives from the gaussian integration over the auxiliary field. From this we find the following condition on the mean bosonic action as a consequence of the scalar supersymmetry

$$\frac{2}{3N_G N_s} \langle \beta S_B \rangle = 1 \quad (5.2)$$

To examine this quantity in the continuum limit we must know how to scale the lattice coupling β with the number of lattice points. Clearly the physics of the model is determined by the *dimensionless* coupling $\mu = g^2 A$ where A is the physical area. If we simply equate this to the corresponding lattice quantity we find the scaling

$$\beta = \frac{L^2}{\mu}$$

The continuum limit is thus gotten from this equation taking $L \rightarrow \infty$ while holding μ fixed. Notice that the infinite volume limit corresponds then to taking the subsequent limit $\mu \rightarrow \infty$.

Figure 1 shows a plot of this quantity for the $SU(3)$ gauge group for $\mu = 0.25$ and $\mu = 5.0$ as the continuum limit is approached with $L = 3, 4, 5$. While small deviations of order 1.5% are seen from the theoretical result based on exact supersymmetry on the smallest lattice with $\mu = 0.25$ these appear to diminish as the continuum limit is taken. Furthermore, at $\mu = 5.0$ the data appears consistent with exact supersymmetry for all

	$SU(2)$		$SU(3)$	
L	B	F	B	F
3	0.031(2)	-0.032(2)	0.13(2)	-0.13(2)
4	0.0087(8)	-0.0094(6)	0.053(9)	-0.055(9)
5	0.0032(5)	-0.0038(6)	0.0091(9)	-0.0109(8)

Table 1: QO_1 vs L for $SU(2)$, $SU(3)$ and $\mu = 0.25$

	$SU(2)$		$SU(3)$	
L	B	F	B	F
3	0.0334(7)	-0.0363(5)	0.077(3)	-0.083(4)
4	0.0215(3)	-0.0222(2)	0.049(3)	-0.051(2)
5	0.016(1)	-0.0146(1)	0.036(1)	-0.0382(2)

Table 2: QO_2 vs L for $SU(2)$, $SU(3)$ and $\mu = 0.25$

	$SU(2)$		$SU(3)$	
L	B	F	B	F
3	0.085(3)	-0.0808(3)	0.21(1)	-0.2172(5)
4	0.046(2)	-0.0460(3)	0.11(1)	-0.1232(4)
5	0.029(3)	-0.0295(1)	0.081(6)	-0.0790(4)

Table 3: QO_3 vs L for $SU(2)$, $SU(3)$ and $\mu = 0.25$

lattice sizes (the maximum deviation being 0.5%). We can easily derive other Ward identities associated with the Q -symmetry by taking the Q -variation of the following operators $O_1(x) = \eta^\dagger(x)[\phi(x), \eta(x)]$, $O_2(x) = \chi_{12}^\dagger(x)F_{12}(x)$ and $O_3(x) = \psi_\mu^\dagger(x)D_\mu\bar{\phi}(x)$. In practice we have examined the integrated quantities $\sum_x O_i(x)$ and estimated the latter by selecting a source point x randomly on each Monte Carlo configuration. Such a procedure minimizes the statistical errors for a fixed amount of computation. After Q -variation we find

$$\begin{aligned}
QO_1 &= [\phi, \bar{\phi}]^2 - \eta^\dagger[\phi, \eta] \\
QO_2 &= F_{\mu\nu}^\dagger(x)F_{\mu\nu}(x) - \chi_{\mu\nu}^\dagger D_{[\mu}^+ \psi_{\nu]} \\
QO_3 &= -D_\mu^+ \phi D_\mu^+ \bar{\phi} - \psi_\mu^\dagger D_\mu^+ \eta - \psi_\mu^\dagger [\bar{\psi}_\mu, \phi]
\end{aligned} \tag{5.3}$$

The results for the expectation values of these Q -variations as a function of lattice size $L = 3, 4, 5$ are shown in tables 1, 2 and 3. for $\mu = 0.25$ and gauge groups $SU(2)$ and $SU(3)$. Similar data at $\mu = 10.0$ (for $SU(2)$) and $\mu = 5.0$ (for $SU(3)$) are shown in tables 4, 5, and 6. We denote the bosonic contribution to the Ward identity by B and the real part of the fermionic contribution by F – the imaginary part is always small and statistically consistent with zero. To give a more graphical illustration of the presence of the exact scalar supersymmetry Q we show in figure 2 plots of $B + F$ versus L for $\mu = 0.25, 5.0$ and gauge group $SU(3)$. In general we see that these Ward identities are rather well satisfied

	$SU(2)$		$SU(3)$	
L	B	F	B	F
3	2.7(2)	-2.8(3)	3.8(1)	-3.9(1)
4	0.81(3)	-0.91(3)	1.12(4)	-1.16(3)
5	0.39(1)	-0.44(1)	0.50(2)	-0.55(2)

Table 4: QO_1 vs L for $SU(2)$ ($\mu = 10.0$) and $SU(3)$ ($\mu = 5.0$)

	$SU(2)$		$SU(3)$	
L	B	F	B	F
3	1.05(8)	-1.07(8)	1.27(4)	-1.31(4)
4	0.755(9)	-0.777(6)	1.00(2)	-1.003(7)
5	0.51(3)	-0.53(2)	0.67(1)	-0.686(5)

Table 5: QO_2 vs L for $SU(2)$ ($\mu = 10.0$) and $SU(3)$ ($\mu = 5.0$)

	$SU(2)$		$SU(3)$	
L	B	F	B	F
3	3.40(8)	-3.24(2)	4.51(5)	-4.36(1)
4	1.87(2)	-1.812(3)	2.46(4)	-2.454(2)
5	1.165(9)	-1.162(2)	1.570(30)	-1.590(10)

Table 6: QO_3 vs L for $SU(2)$ ($\mu = 10.0$) and $SU(3)$ ($\mu = 5.0$)

for all lattice sizes and certainly as we move toward the continuum limit.

5.2 The broken supersymmetries

In this section we examine Ward identities corresponding to the supersymmetries which are broken after discretization. Referring to the previous section we see that these supercharges in general will transform a field living on one link to a neighboring link in a manner similar to the link constructions used in [6]. This in turn implies that the variation of any closed, gauge invariant loop will vary into an open gauge variant loop. The latter will *automatically* have vanishing expectation value due to gauge invariance. Thus the set of operators whose variation under one of these link supersymmetries yields a non-trivial Ward identity is rather small and is further constrained by the need to obtain singlets under the additional $U(1)$ symmetry described in eqn. 2.10. We have examined the following ones

$$Q_{12}O_4 = Q_{12} \left(\chi_{12}^\dagger[\phi, \bar{\phi}] \right) = \frac{1}{4}[\phi, \bar{\phi}]^2 - \chi_{12}^\dagger[\phi, \chi_{12}] \quad (5.4)$$

$$Q_1O_5 = Q_1 \left(\psi_1^\dagger[\phi, \bar{\phi}] \right) = \frac{1}{4}[\phi, \bar{\phi}]^2 - \psi_1^\dagger[\psi_1, \bar{\phi}] \quad (5.5)$$

$$Q_2O_6 = Q_2 \left(\psi_2[\phi, \bar{\phi}] \right) = \frac{1}{4}[\phi, \bar{\phi}]^2 - \psi_2^\dagger[\psi_2, \bar{\phi}] \quad (5.6)$$

	$SU(2)$		$SU(3)$	
L	B	F	B	F
3	0.077(6)	-0.0053(5)	0.032(4)	-0.028(4)
4	0.0022(2)	-0.0013(1)	0.013(3)	-0.012(3)
5	0.0008(1)	-0.0004(1)	0.0023(2)	-0.0018(2)

Table 7: $Q_{12}O_4$ vs L for $SU(2)$, $SU(3)$ for $\mu = 0.25$

	$SU(2)$		$SU(3)$	
L	B	F	B	F
3	0.077(6)	-0.066(6)	0.032(4)	-0.030(4)
4	0.0022(2)	-0.018(1)	0.013(3)	-0.013(2)
5	0.0008(1)	-0.0007(1)	0.0023(2)	-0.0023(2)

Table 8: Q_1O_5 vs L for $SU(2)$, $SU(3)$ for $\mu = 0.25$

	$SU(2)$		$SU(3)$	
L	B	F	B	F
3	0.67(8)	-0.6(1)	0.95(3)	-0.92(4)
4	0.204(7)	-0.161(6)	0.28(1)	-0.25(1)
5	0.099(3)	-0.072(2)	0.124(6)	-0.114(5)

Table 9: $Q_{12}O_4$ vs L for $SU(2)$ ($\mu = 10.0$) and $SU(3)$ ($\mu = 5.0$)

They correspond to terms in the lattice action. Notice that they imply that the expectation values of different Yukawa interactions should be equal. Tables 7 and 8 show data for $SU(2)$ and $SU(3)$ and lattice sizes $L = 3, 4, 5$ at $\mu = 0.25$. Similar data for $SU(2)$ at $\mu = 10.0$ and $SU(3)$ at $\mu = 5.0$ are shown in tables 9 and 10. The results for the Ward identity Q_2O_6 are very similar to those for Q_1 and we omit them. Some of this data is also shown graphically in figures 3 and 4 which again plot $B + F$ against L for $SU(3)$ at $\mu = 0.25, 5.0$ for the operators O_4 and O_5 .

We see no statistically significant evidence for breaking of these Ward identities in these tables *except* for the case of $Q_{12}O_4$ and gauge group $SU(2)$. In this case the breaking appear worse for small μ and appear to survive the continuum limit $L \rightarrow \infty$. We conjecture that the explanation for these breakings lies in the use of the phase quenched approximation. In the next section we examine this issue more carefully and find evidence that the problem of phase fluctuations gets worse at small μ . Moreover, since the latter are driven by near zero modes of the fermion operator it is also plausible that the effect is enhanced for small N since the number of fermionic zero modes scales as N while the number of non zero modes varies as N^2 .

	$SU(2)$		$SU(3)$	
L	B	F	B	F
3	0.67(8)	-0.64(7)	0.95(3)	-0.95(3)
4	0.204(7)	-0.193(6)	0.28(1)	-0.26(9)
5	0.099(3)	-0.092(3)	0.124(6)	-0.123(5)

Table 10: Q_1O_5 vs L for $SU(2)$ ($\mu = 10.0$) and $SU(3)$ ($\mu = 5.0$)

5.3 Phase quenching

In this section we try to quantify the magnitude of any corrections to the Ward identities due to phase quenching. Initially we focus on lattices employing periodic boundary conditions on all fields. Tables 11 and 12 show the cosine of the phase $\langle \cos \alpha \rangle$ for the $SU(2)$ theory at $\mu = 0.25$ and $\mu = 10.0$ respectively. Notice that discretization effects appear to

L	$\langle \cos \alpha \rangle$
3	0.14(1)
4	0.13(2)
5	0.14(4)

Table 11: $SU(2)$ $\mu = 0.25$

L	$\langle \cos \alpha \rangle$
3	0.33(6)
4	0.37(1)
5	0.27(1)

Table 12: $SU(2)$ $\mu = 10.0$

be small and that the mean value increases with increasing μ . A plot of the distribution $P(\cos \alpha)$ for $SU(2)$ from simulations at $L = 3$ and $\mu = 0.25$ is shown in figure 5. A similar picture for $\mu = 10.0$ is plotted in figure 6. From this figure we see that the distribution possesses two peaks - one at $\cos \alpha = 1$ and another at $\cos \alpha = -1$. Thus the measured Pfaffian is predominately real but has an indefinite sign. From the observed weak dependence of $\langle \cos \alpha \rangle$ on L and direct observation of the distribution $P(\cos \alpha)$ at increasing L we conclude that these phase fluctuations survive the continuum limit for any fixed μ . Notice though that the height of the $\cos \alpha = -1$ peak *decreases* relative to the $\cos \alpha = 1$ peak as μ increases which is responsible for the observed increase of $\langle \cos \alpha \rangle$ with μ . We conjecture that the phase becomes concentrated at $\cos \alpha = 1$ in the infinite volume limit corresponding to $\mu \rightarrow \infty$. In this limit then the phase quenched approximation would be exact.

Furthermore, we conjecture that neglect of these phase fluctuation is the origin of the breaking of the Q_{12} Ward identity observed in the previous section for the $SU(2)$ theory at small μ . We have attempted to check this by examining the reweighted values of the bosonic action. The data is shown in table 13 which shows $\langle S_B \rangle$ and its reweighted cousin S_B^R as a function of μ from simulations of the $SU(2)$ theory with $L = 3$.

While the measured value of the reweighted action has very large errors there is an indication that it lies closer to the exact value relative to the unweighted action at small μ . Notice again though that even the naive mean action appears to approach the expected theoretical value for sufficiently large μ .

To summarize we have observed non-trivial fluctuations in the phase of the Pfaffian which appear to survive the continuum limit for any finite continuum coupling μ . These phase fluctuations appear to become less important in the infinite volume limit corresponding to $\mu \rightarrow \infty$.

We conjecture that this non-trivial phase is associated primarily with the fluctuations of lowest lying eigenvalues of the fermion operator. We have directly observed such states which correspond to the superpartners of the bosonic zero modes associated with the classical moduli space. One simple way to try to reduce the problem is to consider the theory at finite temperature by employing *antiperiodic* temporal boundary conditions on the fermions. We consider this in detail in the next section.

μ	S_B	S_B^R
0.25	0.977(1)	0.989(70)
1.0	0.981(1)	0.995(45)
5.0	0.992(2)	1.000(32)
10.0	0.999(2)	1.003(160)

Table 13: S_B and reweighted S_B^R vs μ for $SU(2)$ and $L = 3$

5.4 Thermal boundary conditions

In tables 14 and 15 we show the measured values of $\langle \cos \alpha \rangle$ versus L for couplings $\mu = 0.25$ and $\mu = 10.0$ from thermal simulations using gauge group $SU(2)$. Notice that the use of thermal boundary conditions does indeed push the distribution toward $\cos \alpha = 1$. This is consistent with the effect being driven primarily by the near zero modes whose eigenvalues are lifted to $O(1/L)$ at finite temperature. The distribution for $\mu = 10.0$ in the $SU(2)$ theory at $L = 3$ is shown in figure 7. In this case the distribution is essentially zero away from a very sharp peak at $\cos \alpha = 1$ whose width is only $O(0.01)$. Notice, however, that this peak broadens as the continuum limit is approached and the expectation value of $\cos \alpha$ subsequently falls. We have repeated the calculations of the supersymmetric Ward

L	$\langle \cos \alpha \rangle$
3	0.86(8)
4	0.86(3)
5	0.72(5)

Table 14: $SU(2)$ apbc $\mu = 0.25$

L	$\langle \cos \alpha \rangle$
3	0.95(2)
4	0.79(5)
5	0.50(1)

Table 15: $SU(2)$ apbc $\mu = 10.0$

identities for the thermal case and the results for QO_1 , $Q_{12}O_4$ and Q_1O_5 are shown in tables 16, 17 and 18 at couplings $\mu = 10.0$ for $SU(2)$ and $\mu = 5.0$ for $SU(3)$. For the thermal runs we are interested primarily in the data for large coupling μ which is now related to the inverse temperature - thus large μ corresponds to the theory at low temperature and/or large spatial volume. The data is also illustrated graphically in figure 8 for the case of $SU(3)$. In this regime we find that all the supersymmetric Ward identities computed within the phase quenched approximation are satisfied within statistical errors - thus we conclude that the use of thermal boundary conditions may indeed be quite useful in reducing phase fluctuation problems and eliminating the need for reweighting even away from the infinite volume limit.

In the absence of spontaneous supersymmetry breaking expectation values computed in the thermal system should approach those of the periodic/zero temperature theory for

	$SU(2)$		$SU(3)$	
L	B	F	B	F
3	4.2(2)	-4.2(2)	5.2(3)	-5.3(2)
4	1.8(2)	-1.8(2)	2.1(1)	-2.1(1)
5	0.53(2)	-0.55(2)	0.90(8)	-0.93(8)

Table 16: QO_1 for $SU(2)$ with apbc ($\mu = 10.0$) and $SU(3)$ ($\mu = 5.0$)

	$SU(2)$		$SU(3)$	
L	B	F	B	F
3	1.05(5)	-1.03(6)	1.30(6)	-1.29(6)
4	0.45(5)	-0.42(6)	0.53(3)	-0.50(4)
5	0.132(6)	-0.101(6)	0.22(2)	-0.21(2)

Table 17: $Q_{12}O_4$ for $SU(2)$ with apbc ($\mu = 10.0$) and $SU(3)$ ($\mu = 5.0$)

	$SU(2)$		$SU(3)$	
L	B	F	B	F
3	1.05(5)	-1.03(6)	1.30(6)	-1.31(6)
4	0.45(5)	-0.44(5)	0.53(3)	-0.51(3)
5	0.132(6)	-0.119(5)	0.22(2)	-0.22(2)

Table 18: Q_1O_5 for $SU(2)$ with apbc ($\mu = 10.0$) and $SU(3)$ ($\mu = 5.0$)

sufficiently low temperatures. No additional fine tuning should be required and this is seen in our data for the Ward identities.

5.5 Rotational invariance

To test for a restoration of rotational invariance as β is increased and the continuum limit is approached we have examined the two-point function

$$G(x, y) = \langle B(0, 0)B(x, y) \rangle \quad (5.7)$$

where $B(x, y) = [\phi(x, y), \bar{\phi}(x, y)]$ and x and y are integer lattice coordinates. If the theory is rotationally invariant we would expect this correlator to be a function of just the radial distance $r = \sqrt{x^2 + y^2}$. Figure 9. shows a plot of this function for the $SU(2)$ theory at $\beta = 8.0$ on a 8×8 lattice. The points lie within errors on a single curve lending support to the idea that at least the scalar sector of the theory is rotationally invariant at large distance. If all supersymmetries are restored for sufficiently small lattice spacing we would then expect the fermionic sector to also be rotationally invariant in the continuum limit. Fig 10 shows similar data for $SU(3)$ at $\beta = 4.0$ and leads to similar conclusions.

5.6 Fluctuations of the scalar fields

The classical vacua of this theory allow for any set of scalars which are constant over the lattice and satisfy

$$[\phi, \bar{\phi}] = 0 \quad (5.8)$$

In the case of $SU(2)$ and using the parameterization $\phi = \phi_1 + i\phi_2$ we find vacuum states of the form

$$\phi_1 = (A, 0, 0) \quad \phi_2 = (B, 0, 0) \quad (5.9)$$

together with global $SU(2)$ rotations of this configuration. Thus we have a classical vacuum state for any value of A and B . In the case of $SU(3)$ the general vacuum state can be realized by taking the fields ϕ_1 and ϕ_2 as constant diagonal matrices with arbitrarily large matrix elements. Generalization to arbitrary $SU(N)$ the space of vacuum solutions is referred to as the classical moduli space. The presence of such a non-trivial moduli space corresponds to the existence of flat directions in the theory which have the potential to lead to divergences when inserted into a path integral. Notice, however, that the fermion operator develops zero modes precisely along these bosonic flat directions and thus quantum fluctuations of the fermions may suppress their contribution. In addition, entropic effects at large N may also play a role in removing potential divergences since the number of classical zero modes scales like N while the number of non-zero modes scales like N^2 . It then becomes a dynamical question as to whether the theory retains a non-trivial moduli space at the quantum level.

To examine this issue we have measured the probability distribution of the scalar eigenvalues seen in the simulation. Figure 11. shows a plot of this distribution of scalar field eigenvalues for $SU(2)$ obtained from high statistics runs (10^5 Monte Carlo trajectories) on a 3×3 lattice. We have mapped all data to positive values by exploiting the $\lambda \rightarrow -\lambda$ symmetry of the action. The two sets of points correspond to $\beta = 0.5$ and $\beta = 4.0$. Contrary to the classical analysis it appears that the most probable scalar field configurations lie close to the origin in field space and this effect is enhanced as the coupling β is increased. A similar situation is seen for $SU(3)$ in figure 12. – the main difference being that there are now three peaks in this distribution (only two are seen after the mapping to the positive λ axis) with a new peak appearing at the origin. This pattern repeats at larger N – in the case of $SU(N)$ we have observed that this probability distribution possesses N peaks [17]. Since the scalars in this theory arise from dimensional reduction of gauge fields in four dimensional $\mathcal{N} = 1$ Yang-Mills it seems likely that these N peaks in the scalar distribution are analogous to the N peaks appearing in the distribution of the expectation value of the Polyakov line in the usual deconfined phase of lattice gauge theory.

At first glance these plots suggest that the scalars are driven to the origin as $\beta \rightarrow \infty$ (or equivalently $L \rightarrow \infty$ at fixed μ) and the quantum continuum theory possesses only the trivial vacuum state $\langle \phi \rangle = 0$. However, we must be careful as the distributions clearly possess long tails extending out to large eigenvalue. We have examined this issue in more detail and indeed find good evidence for power law behavior in the tails of the distribution – see figure 13. which shows a plot of $\log(P(\lambda))$ versus $\log \lambda$ using data from the tail of the distribution for both $SU(2)$ and $SU(3)$ at a coupling $\beta = 4.0$. The exponent extracted

from a linear fit lies in the range of (minus) 2.1 – 2.3. Such an exponent would clearly lead to a normalizable distribution and hence a convergent partition function⁴. Moreover, since the global $U(1)$ symmetry cannot break in two dimensions, it is clear that the first moment of this distribution $\langle \lambda \rangle$ will vanish. However, a value of $p \leq 3$ would ensure that the variance $\langle \lambda^2 \rangle - \langle \lambda \rangle^2$ is divergent. This can be seen explicitly in our simulations with figure 14. showing the Monte Carlo evolution of λ^2 (averaged over the lattice and the number of colors) for the $\beta = 4$ $SU(2)$ run. We see large fluctuations occurring at intervals of order 10,000 RHMC trajectories. These spikes make it extremely difficult to determine the expectation value of $\langle \lambda^2 \rangle$ – the statistical error does not decrease with the square root of the number of measurements as would be expected for a typical Monte Carlo process. These large spikes in $\langle \lambda^2 \rangle$ are also seen for $\beta = 0.5$ and $\beta = 8.0$.

We conjecture that the existence of these tails is related to the existence of a noncompact classical moduli space. This motivates us to consider the lattice theory in the limit of very large β . In this limit we may restrict our attention to fields which are constant over the lattice and the theory reduces to a zero dimensional matrix model. This model has been studied previously with the result that the eigenvalue distributions again have power law tails with (negative) exponent $p \sim 3$ *independent* of the number of colors N [18].

The results for finite β in the two dimensional models look rather similar. It is tempting to interpret this divergence of the variance $\langle \lambda^2 \rangle - \langle \lambda \rangle^2$ as evidence that quantum effects will destroy any classical vacuum with $\langle \lambda \rangle \neq 0$ - the fluctuations around any such solution will be so large as to swamp the mean value and lead to a restoration of the $\lambda \rightarrow -\lambda$ symmetry.

6. Conclusions

In this paper we have extended our previous numerical study of $\mathcal{N} = 2$ super Yang-Mills theory in two dimensions described in [13]. The discretization we have employed was first proposed in [8] and is based upon mapping the twisted continuum theory into a theory of Kähler-Dirac fields which may then be discretized preserving gauge invariance and a single supersymmetry while simultaneously avoiding problems of fermion doubling. In the previous paper we presented numerical results supporting the existence of an exact scalar supersymmetry Q in the case of the $SU(2)$ theory. In this paper we have derived the action of the remaining twisted supersymmetries on the component Kähler-Dirac fields and studied some non-trivial Ward identities following from those symmetries for both $SU(2)$ and $SU(3)$. It should be noted that many of these additional Ward identities are automatically zero because of gauge invariance and so the additional symmetries supply rather few additional constraints.

Our numerical results, carried out within the phase quenched approximation, support a restoration of *all* supersymmetries in the continuum limit *at least for large continuum dimensionless coupling* $\mu = g^2 A$. Such a limit corresponds to large physical volumes and appears necessary in order to justify the phase quenched approximation which we have, of

⁴Actually since here we use periodic boundary conditions on all fields the partition function is more properly thought of as a Witten index.

necessity, employed. Furthermore, we have shown that an additional suppression of this phase on finite lattices can be achieved by using thermal boundary conditions. We have also examined a correlation function of the scalar fields which shows good evidence of a restoration of rotational invariance at large distances which is also encouraging.

These conclusions are consistent with perturbative arguments based on continuum power counting see for example [10, 5] which argue that a single exact supersymmetry plus gauge invariance and the additional global $U(1)$ symmetry prohibit the occurrence of *relevant* SUSY violating operators as the cut-off is removed.

Finally, we present new results concerning the eigenvalue distributions of the scalar fields. For $SU(2)$ we see two symmetrically disposed peaks in this distribution which narrow and approach the origin as $\beta \rightarrow \infty$. In the case of $SU(3)$ three peaks are seen. This pattern appears to persist at larger N with the distribution showing N peaks. A more detailed analysis reveals power law tails to these distributions which ensures that sufficiently high moments of the eigenvalue distributions will diverge. Our data is consistent with a divergence of the second moment for both $SU(2)$ and $SU(3)$ at least for large β . Such a result is similar to previous results for supersymmetric matrix models [18].

Furthermore, we have argued that the divergent variance would lead to large fluctuations in the scalar fields which would tend to wash out any classical vacuum state with $\langle \phi \rangle \neq 0$. Thus the classical moduli space does not survive in the full quantum theory.

Acknowledgments

This work was supported in part by DOE grant DE-FG02-85ER40237. Many of the numerical calculations were carried out using USQCD resources. The author would like to thank Joel Giedt and Toby Wiseman for useful discussions.

References

- [1] S. Catterall, PoS LAT2005 (2005) 006.
- [2] D. B. Kaplan, Nucl. Phys. B (Proc. Suppl.) 129-130 (2004) 109.
- [3] A. Feo, Nucl. Phys. B. (Proc. Suppl.) 2002.
- [4] S. Catterall, JHEP 0305 (2003) 038.
- [5] F. Sugino, JHEP 0401 (2004) 015
 F. Sugino, JHEP 0403 (2004) 067
 F. Sugino, JHEP 0501 (2005) 016
 F. Sugino, Phys.Lett. B635 (2006) 218-224
- [6] A. D’Adda, I. Kanamori, N. Kawamoto, K. Nagata, Nucl.Phys. B707 (2005) 100-144
 A. D’Adda, I. Kanamori, N. Kawamoto, K. Nagata Phys.Lett. B633 (2006) 645-652.
- [7] K. Ohta and T. Takimi, hep-lat/0611011.
- [8] S. Catterall, JHEP 0411 (2004) 006.
- [9] S. Catterall, JHEP 0506 (2005) 027.

- [10] D.B. Kaplan, E. Katz and M. Unsal, JHEP 0305 (2003) 03
A.G. Cohen, D.B. Kaplan, E. Katz, M. Unsal, JHEP 0308 (2003) 024
A.G. Cohen, D.B. Kaplan, E. Katz, M. Unsal, JHEP 0312 (2003) 031
D. B. Kaplan and M. Unsal, JHEP 0509 (2005) 042.
- [11] M. Unsal, JHEP 0610 (2006) 089.
- [12] J. Giedt, Int.J.Mod.Phys. A21 (2006) 3039-3094
- [13] S. Catterall, JHEP 0603 (2006) 032.
- [14] T. Banks, Y. Dothan, D. Horn, Phys.Lett.B117:413,1982.
- [15] J. Rabin, Nucl. Phys. B201 (1982) 315.
- [16] H. Aratyn, M. Goto and A.H. Zimerman, Nuovo Cimento A84, (1984) 255.
- [17] S. Catterall and T. Wiseman, in preparation.
- [18] W. Krauth and M. Staudacher, Phys.Lett.B453:253-257,1999.

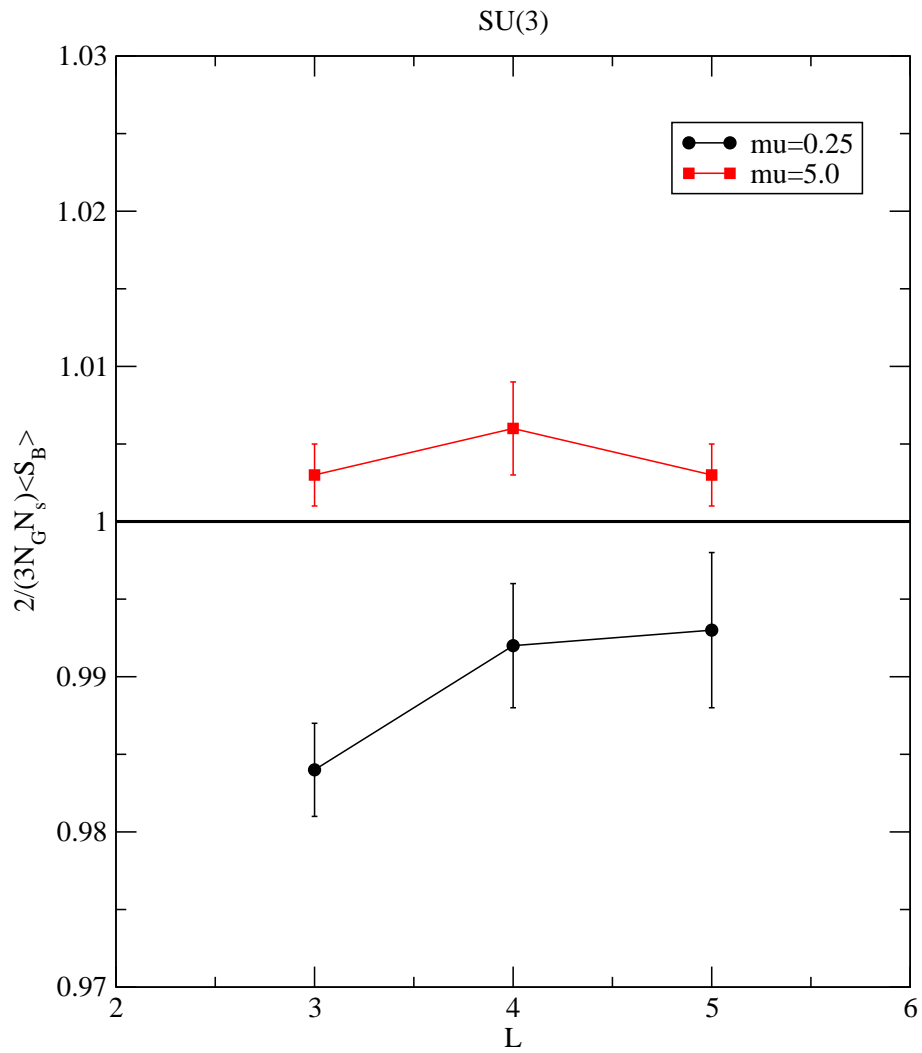


Figure 1: S_B vs L for $SU(3)$ with $\mu = 0.25, 5.0$

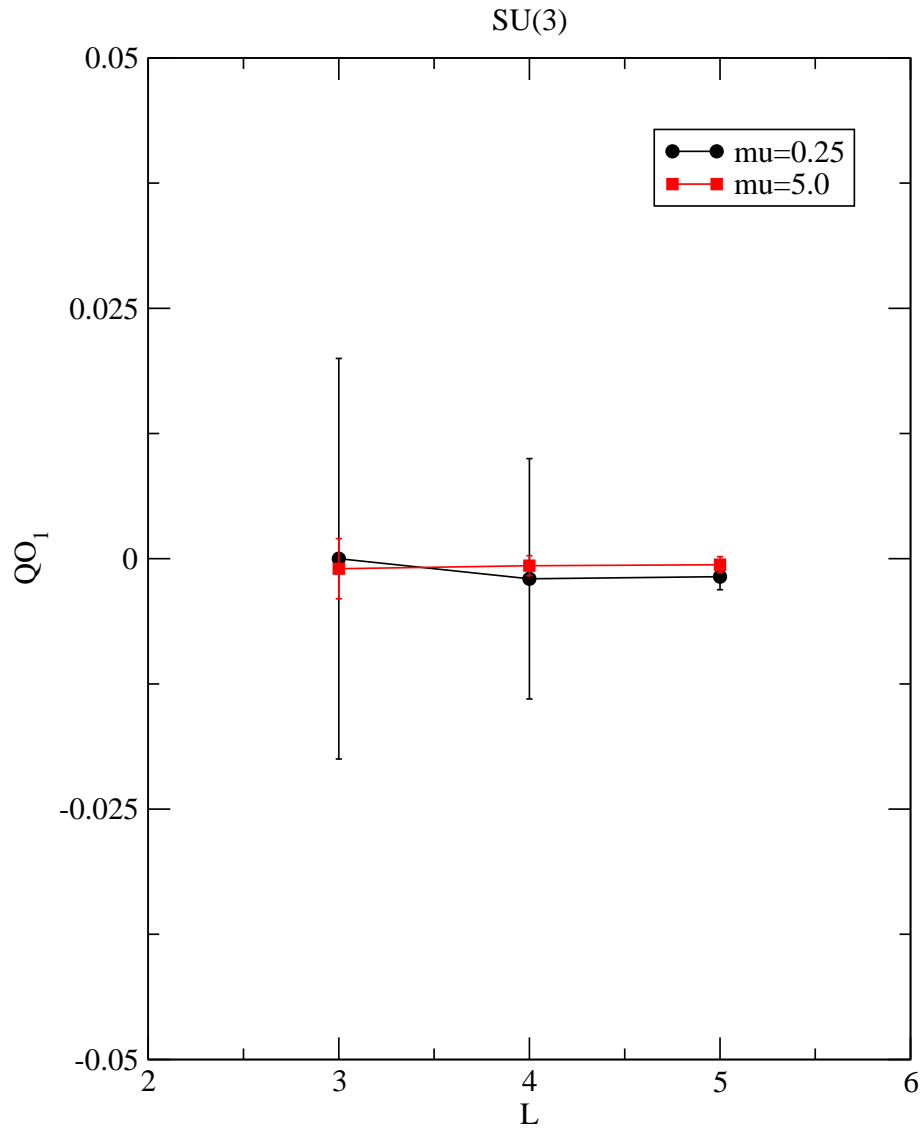


Figure 2: QO_1 vs L for $SU(3)$ with $\mu = 0.25, 5.0$

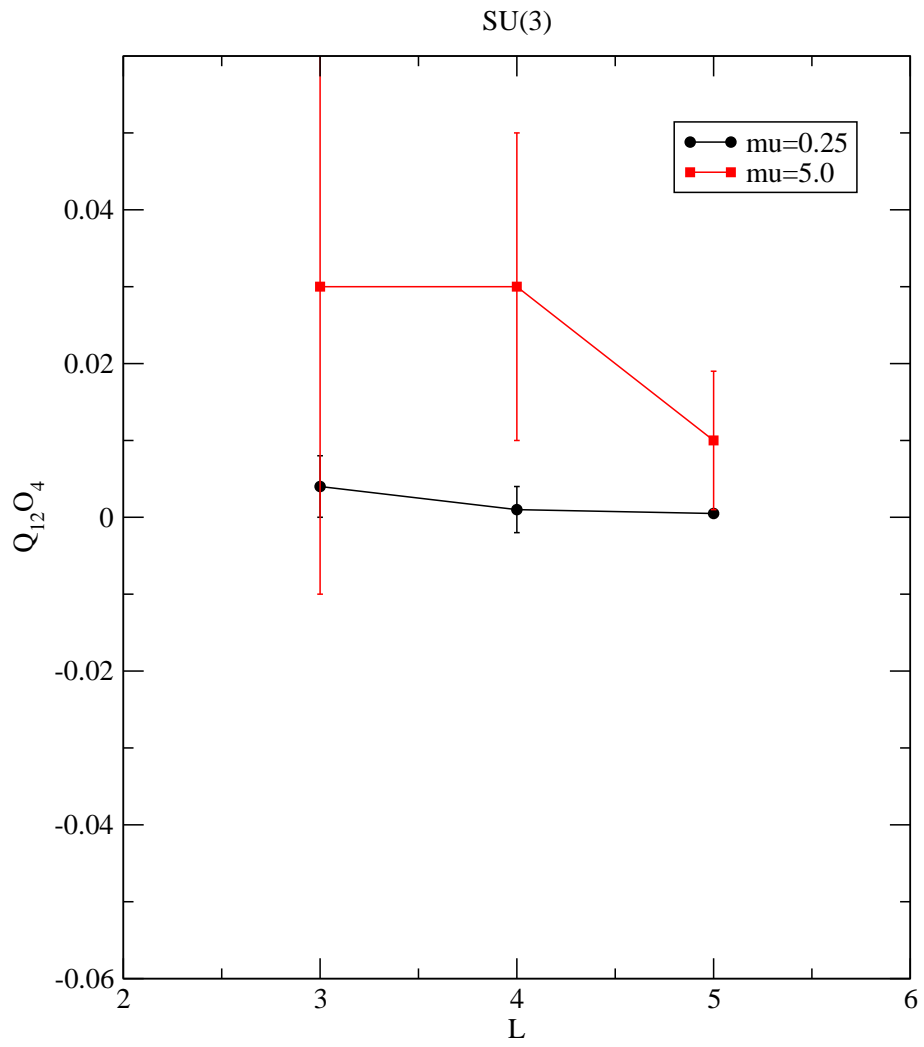


Figure 3: $Q_{12}O_4$ vs L for $SU(3)$ with $\mu = 0.25, 5.0$

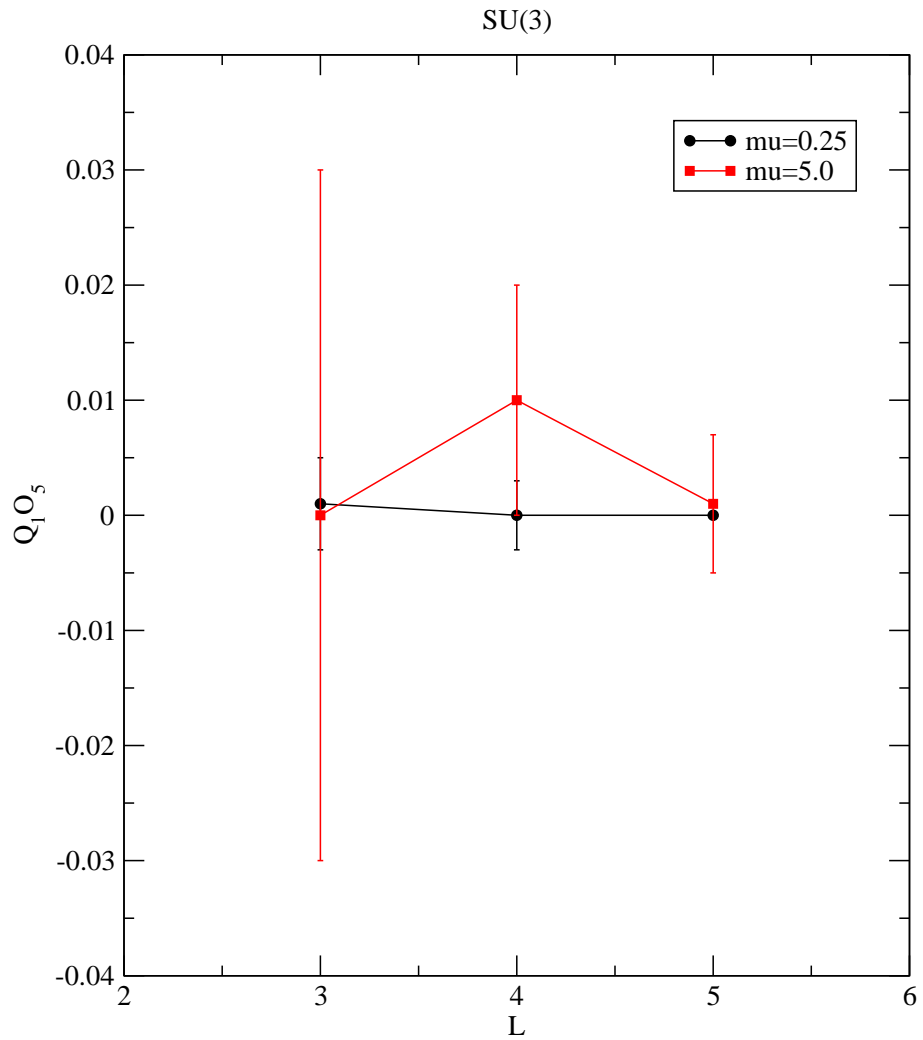


Figure 4: $Q_1 O_5$ vs L for $SU(3)$ with $\mu = 0.25, 5.0$

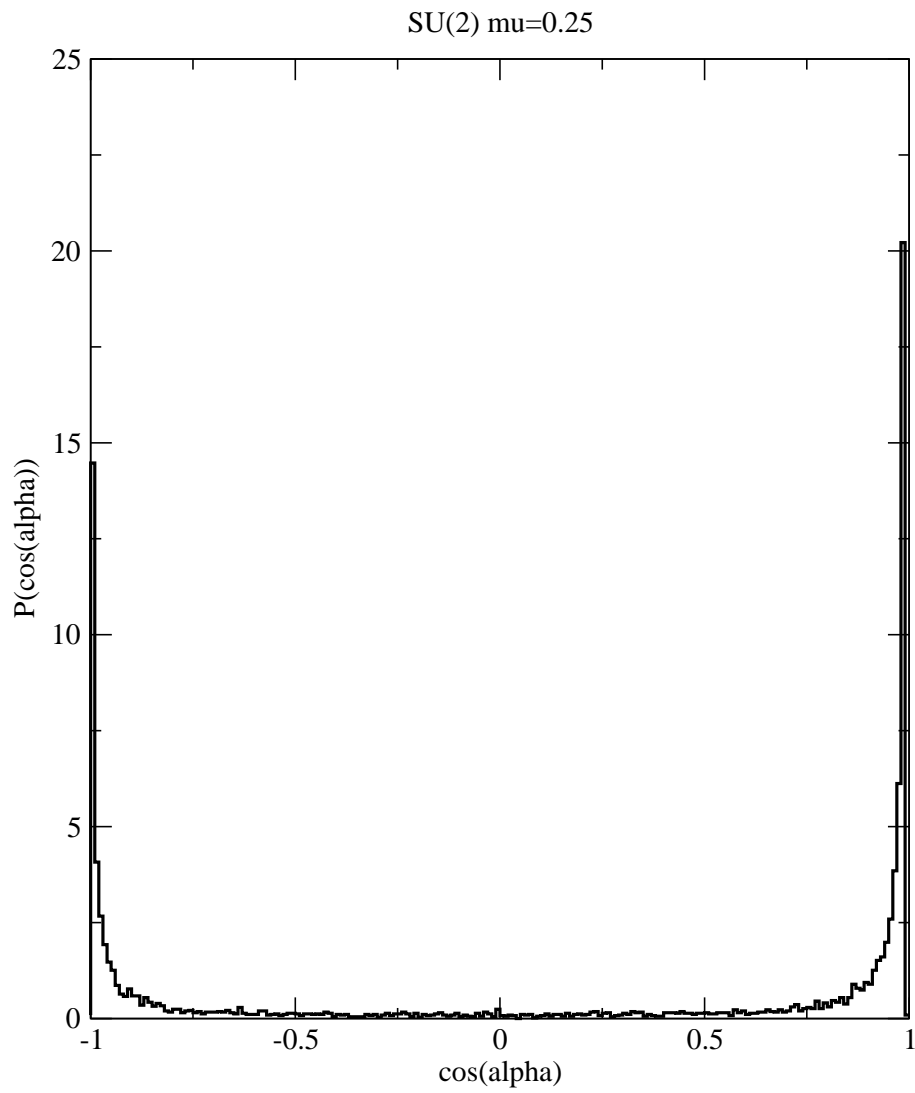


Figure 5: $P(\cos \alpha)$ vs $\cos \alpha$ for $SU(2)$ with $L = 3$ $\mu = 0.25$

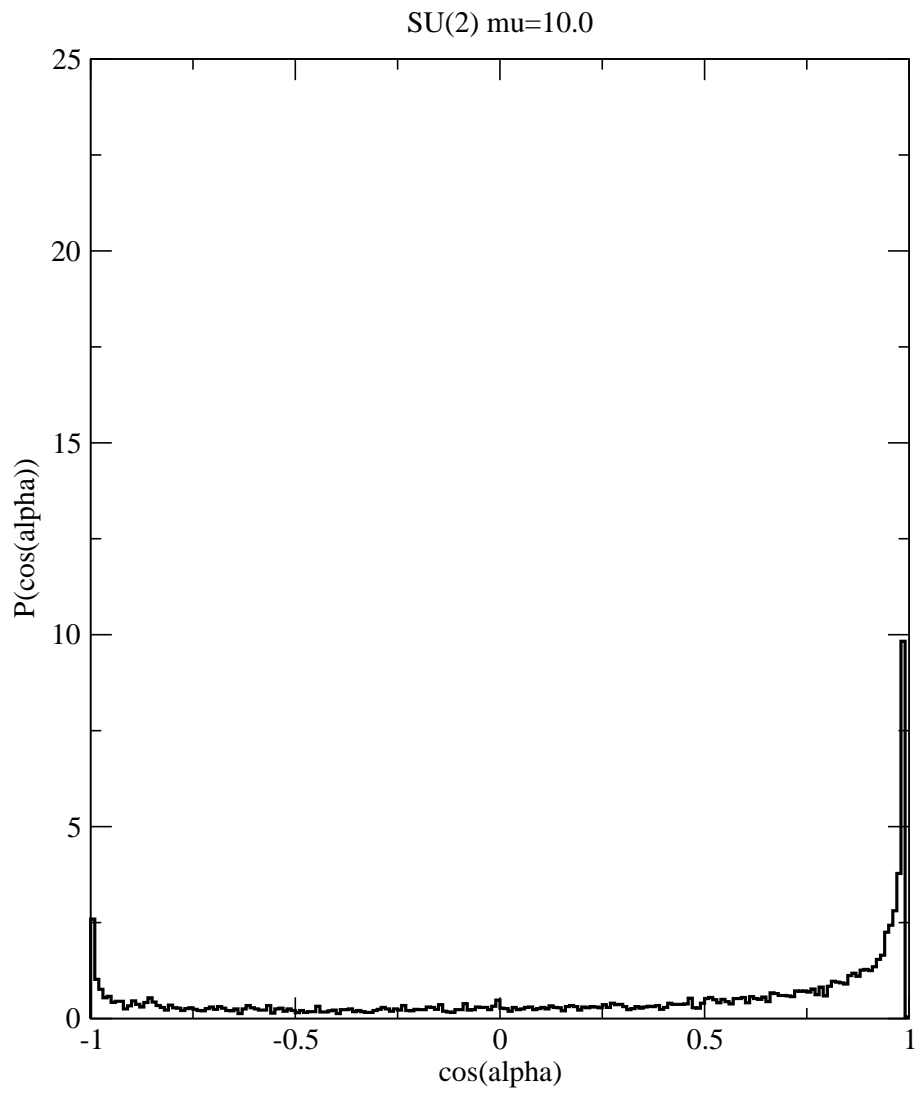


Figure 6: $P(\cos \alpha)$ vs $\cos \alpha$ for $SU(2)$ with $L = 3$ $\mu = 10.0$

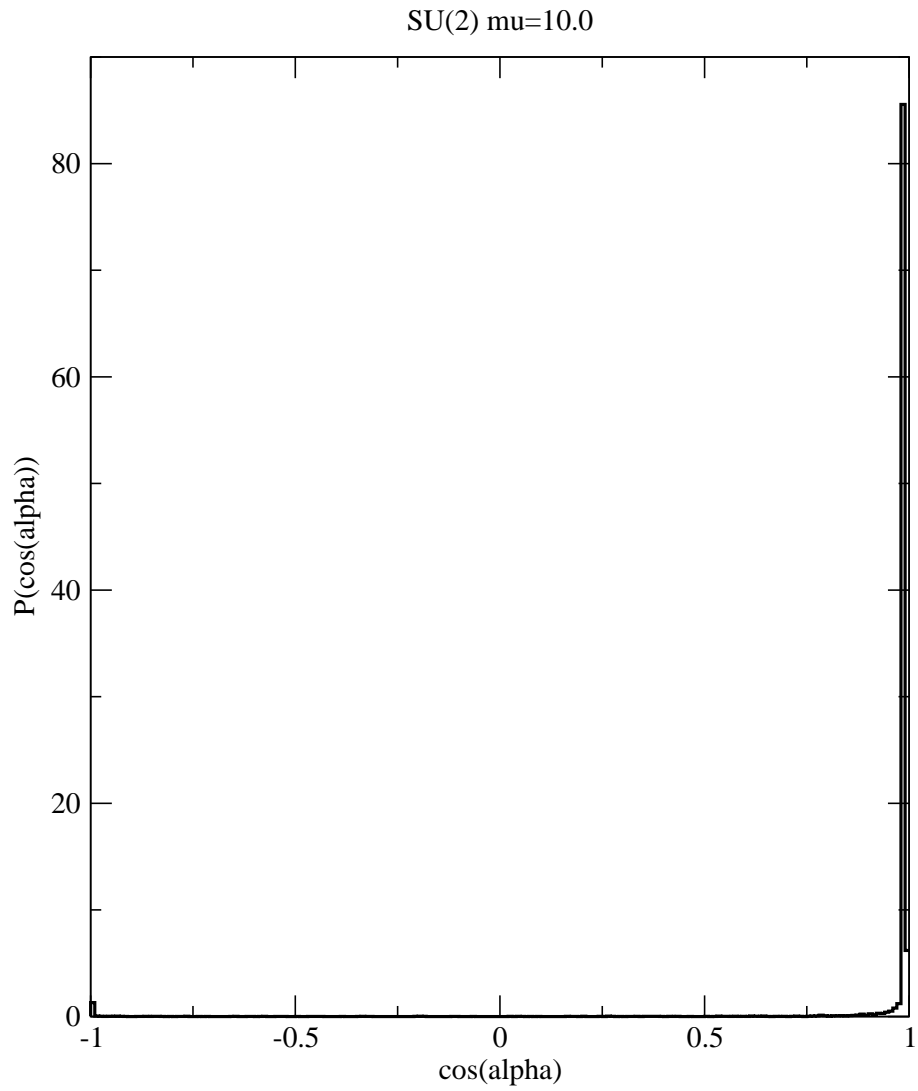


Figure 7: $P(\cos \alpha)$ vs $\cos \alpha$ for thermal $SU(2)$ with $L = 3$ $\mu = 10.0$

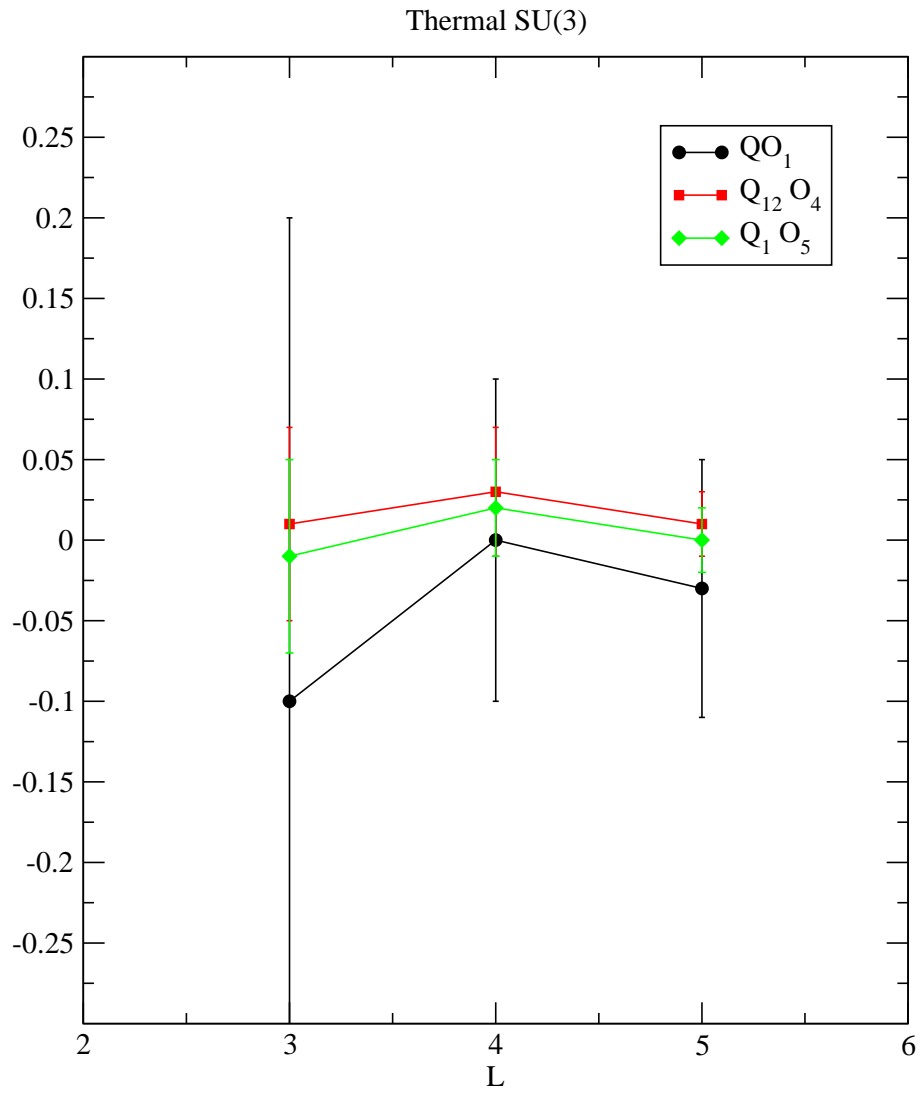


Figure 8: QO_1 , $Q_{12}O_4$ and Q_1O_5 vs L for thermal $SU(3)$ at $\mu = 5.0$

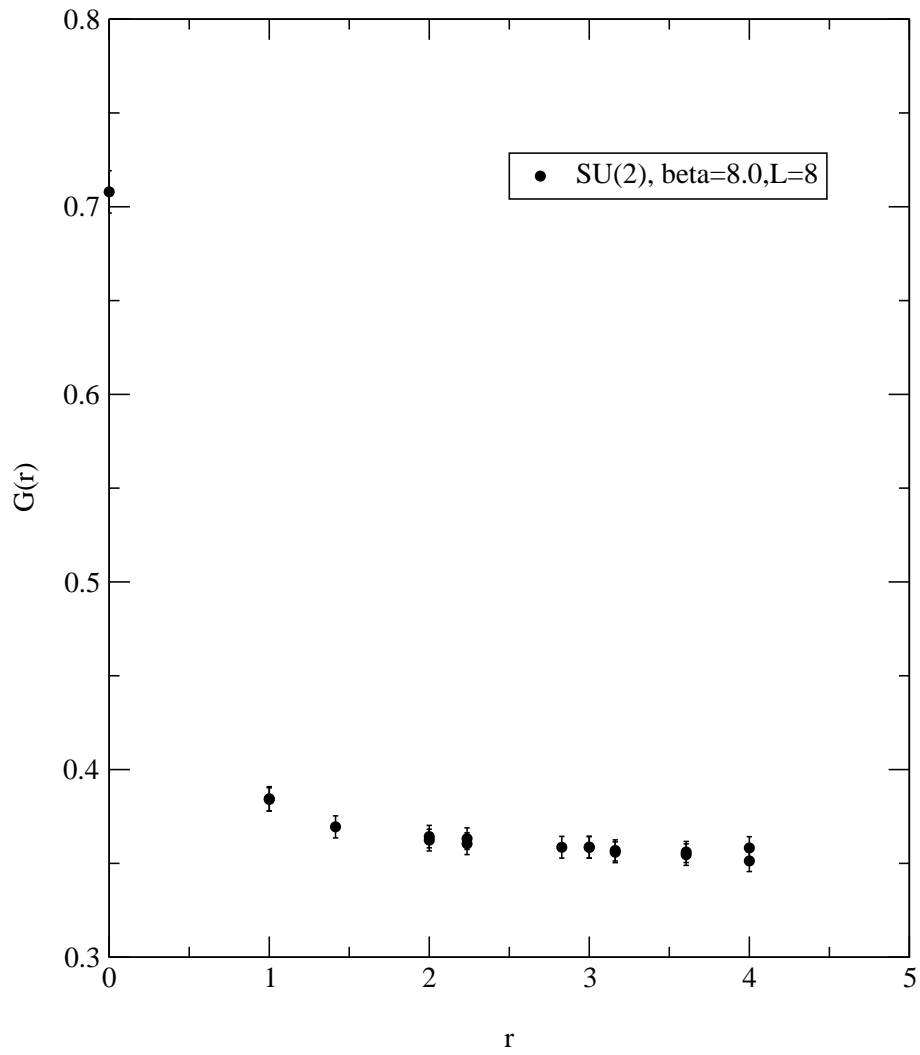


Figure 9: $G(r)$ vs r for $SU(2)$ and $\beta = 8.0$ with $L = 8$

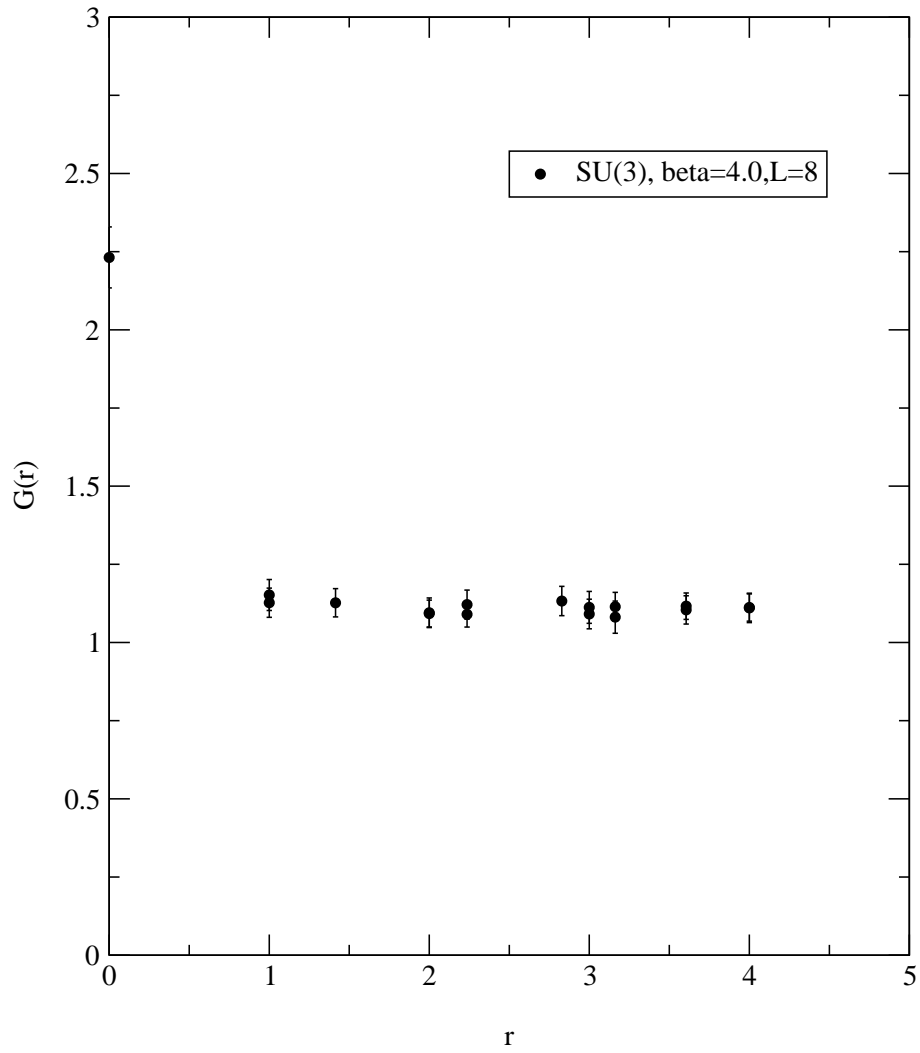


Figure 10: $G(r)$ vs r for $SU(3)$ and $\beta = 8.0$ with $L = 8$

Probability distribution of eigenvalues of scalars
 $SU(2), 3^2$

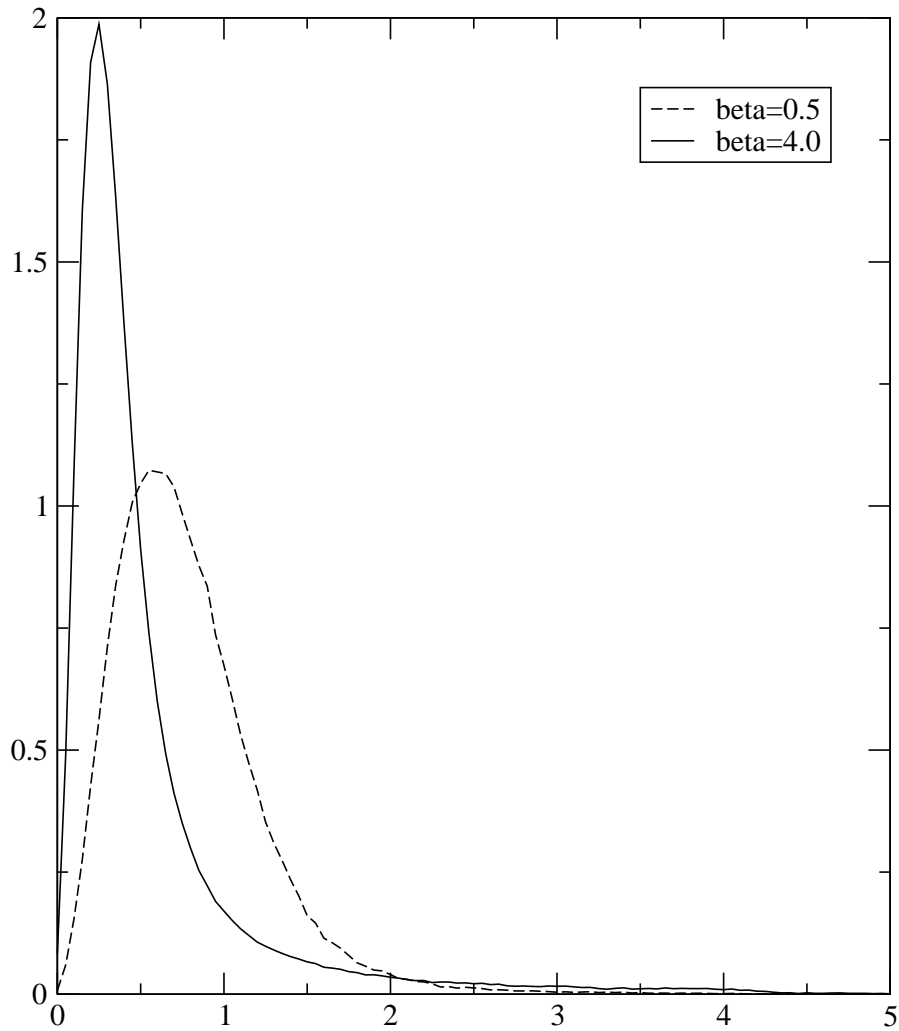


Figure 11: Eigenvalue distribution for $SU(2)$ and $L = 3$

Probability distribution of eigenvalues of scalars
 $SU(3), 3^2$

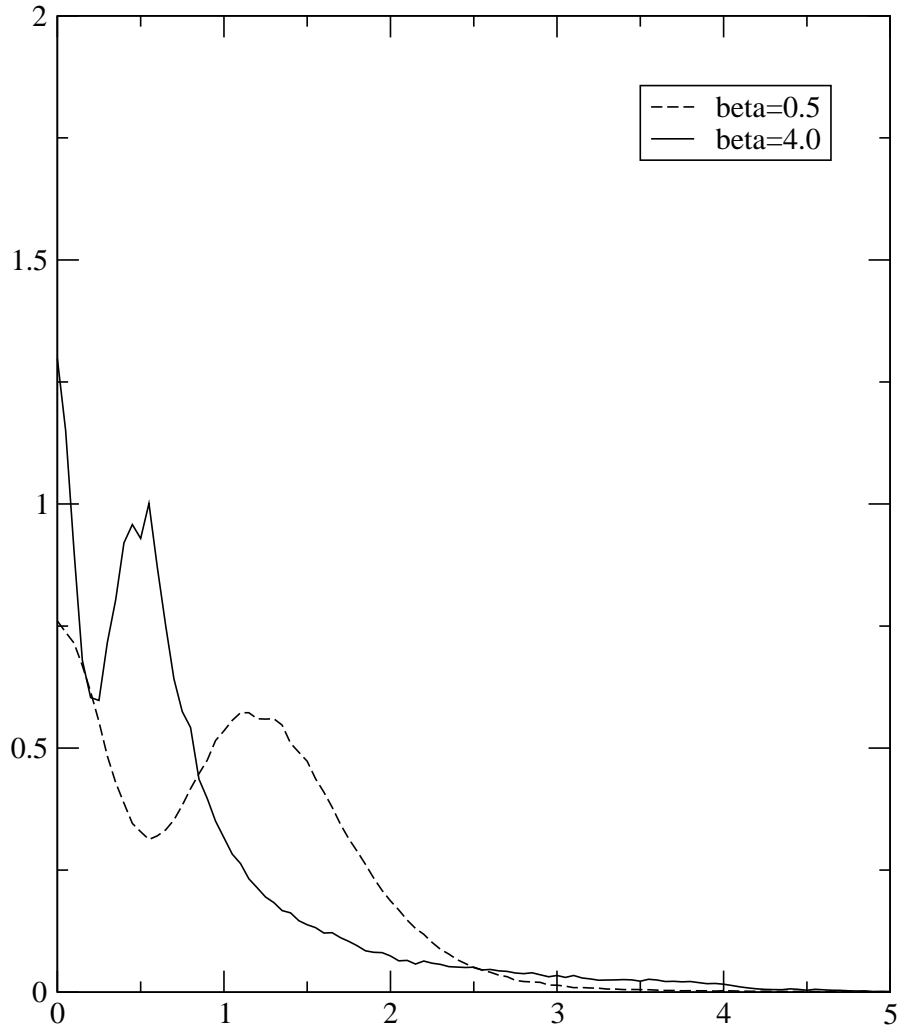


Figure 12: Eigenvalue distribution for $SU(3)$ and $L = 3$

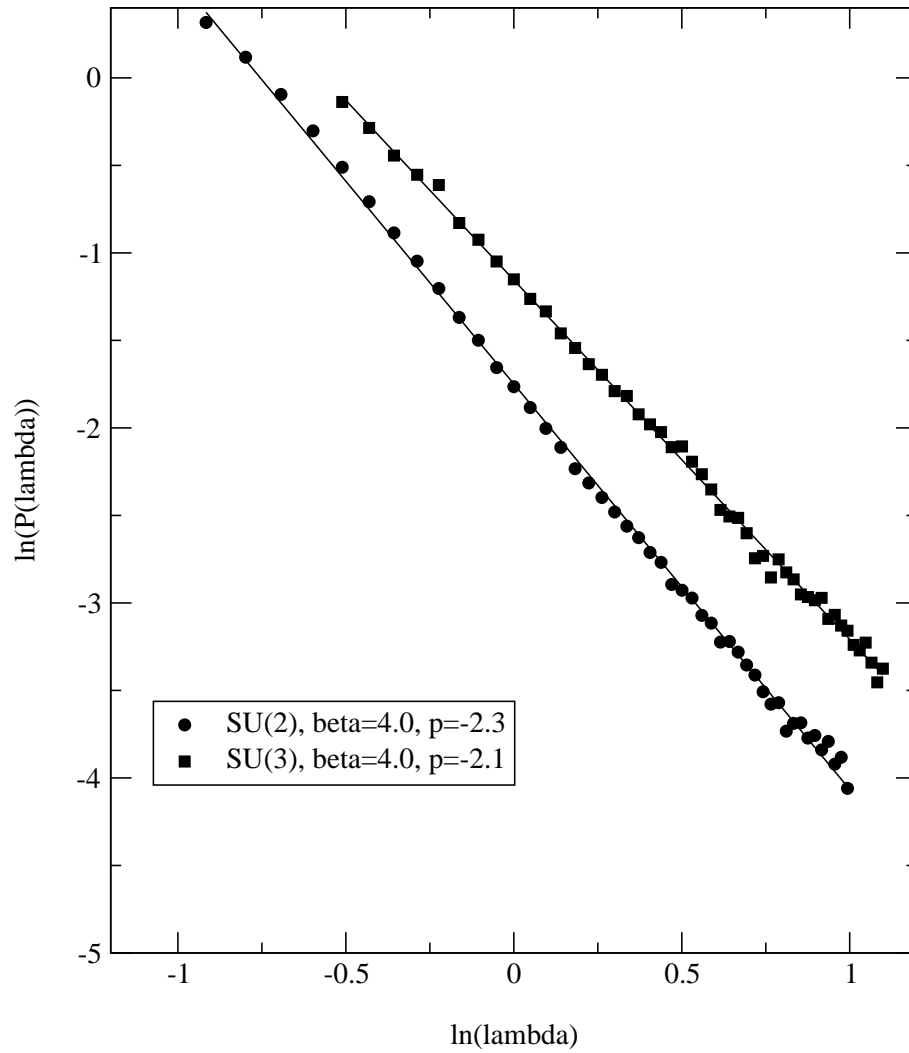


Figure 13: $\log(P(\lambda))$ vs $\log \lambda$ for $L = 3$ and both $SU(2)$ and $SU(3)$

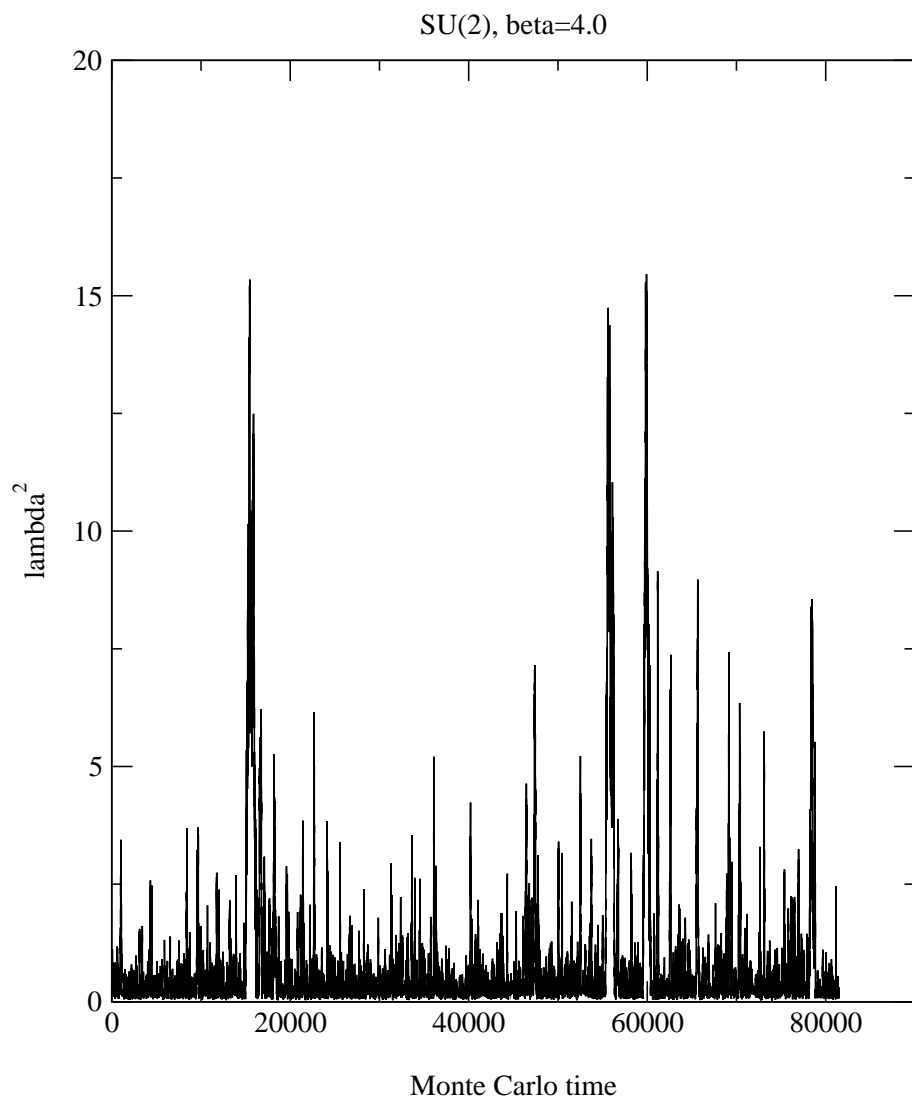


Figure 14: Monte Carlo history for $L = 3$, $\beta = 4.0$ and $SU(2)$